

Highly-ordered aluminosilicate mesoporous mesophase materials: physico-chemical properties and catalytic behaviour

E.G. Kodenev^a, A.N. Shmakov^b, A.Yu. Derevyankin^b, O.B. Lapina^b,
V.N. Romannikov^{b,*}

^a Novosibirsk State University, Novosibirsk, 630090, Russia

^b Boreskov Institute of Catalysis, Novosibirsk, 630090, Russia

Abstract

Structural and textural characteristics as well as coordination states of aluminium and some catalytic properties are studied for highly-ordered (with very narrow XRD reflections) aluminosilicate mesoporous mesophase materials ((Si,Al)-MMM) prepared with different aluminium concentrations by hydrothermal synthesis in the presence of $C_{16}H_{33}N(CH_3)_3Br$. As shown, all physico-chemical parameters measured for these systems including their structural hydrostability are strongly influenced by the aluminium content. Based on analysis of the results obtained, a description of probable transformations during formation of mesoporosity in the C16-(Si,Al)-MMM is considered. © 2000 Elsevier Science B.V. All rights reserved.

Keywords: MCM-41; Mesoporous mesophase materials; Structure; Nitrogen adsorption; ^{27}Al MAS NMR; Benzene alkylation

1. Introduction

In the 1990s, the development of a new direction in nanotechnology of inorganic materials was initiated [1]. It is based on a self-assembling of organized mesophases formed in aqueous solutions of surfactant and appropriate inorganic components. The surfactant removal (for example, by calcination) from a mesophase leads to a mesoporous mesophase material. It has a highly organized long-range order assigned, for example, to hexagonal packing of mesopores of a nanometer range, without

short-range order in an atomic structure of inorganic component (type MCM-41). In the past few years, the investigation of the MCM-41 has been the subject of many papers and reviews [2–4]. One of the major reasons for this interest is their application in acid–base catalysis. Since aluminium is the origin of the acidity in aluminosilicates, the properties of aluminosilicate MCM-41 have been of special interest. However, the materials investigated often had quite broad reflections [5–13] probably due to an inconsistency of their unit cell parameter, which complicates both definite interpretation of their textural characteristics and understanding of the results obtained under studying their physico-chemical properties.

In this paper we analyze structural and textural characteristics of highly-ordered aluminosili-

* Corresponding author. Tel.: +7-383-239-73-14; fax: +7-3832-343056.

E-mail address: zeolite@catalysis.nsk.su (V.N. Romannikov).

cate mesoporous mesophase materials ((Si,Al)-MMM) with different Al concentrations, the coordination state of aluminium atoms, as well as some catalytic properties of these systems. Based on the results obtained, a description of probable physico-chemical transformations during formation of mesoporosity in the (Si,Al)-MMM is considered.

2. Experimental

The C16-(Si,Al)-MMM samples with the [Al/(Si + Al)] atomic ratio varied in the range of 0–0.05 were prepared in the presence of $C_{16}H_{33}N(CH_3)_3Br$ by hydrothermal synthesis at 140°C using water soluble silicates and anionic aluminium complexes (such as $Al(OH)_4^-$, $Al(OR)_4^-$, and others) as sources of silica and alumina, respectively. All the systems were characterized by the XRD using synchrotron radiation and the N_2 adsorption. ^{27}Al MAS NMR spectra were measured at 104.2 MHz and at $\nu_R = 12$ kHz for the samples after their full saturation with water vapour at ambient temperature. Textural parameters were calculated from the adsorption data as described in Ref. [14]. Catalytic experiments were carried out for benzene alkylation with iso-butene for starting molar ratio of (benzene/iso-butene) = 10 in a flow reactor under atmospheric pressure at $150 \pm 3^\circ C$ and $WHSV = 1.2 \pm 0.1$.

3. Results and discussion

The XRD patterns of the C16-(Si,Al)-MMM studied (Fig. 1) are of well-known overall type [2–4], but, unlike most earlier published data [5–13], the reflections observed in this work are of highly-symmetric (Gaussian) shape with the full-width-at-half-maximum (FWHM) values for both as-synthesized and calcined forms about 0.06 – $0.08^\circ 2\theta$ (Fig. 2). The latter is comparable with that for initial synchrotron beam (0.03 – $0.04^\circ 2\theta$). The peculiarities of the XRD pat-

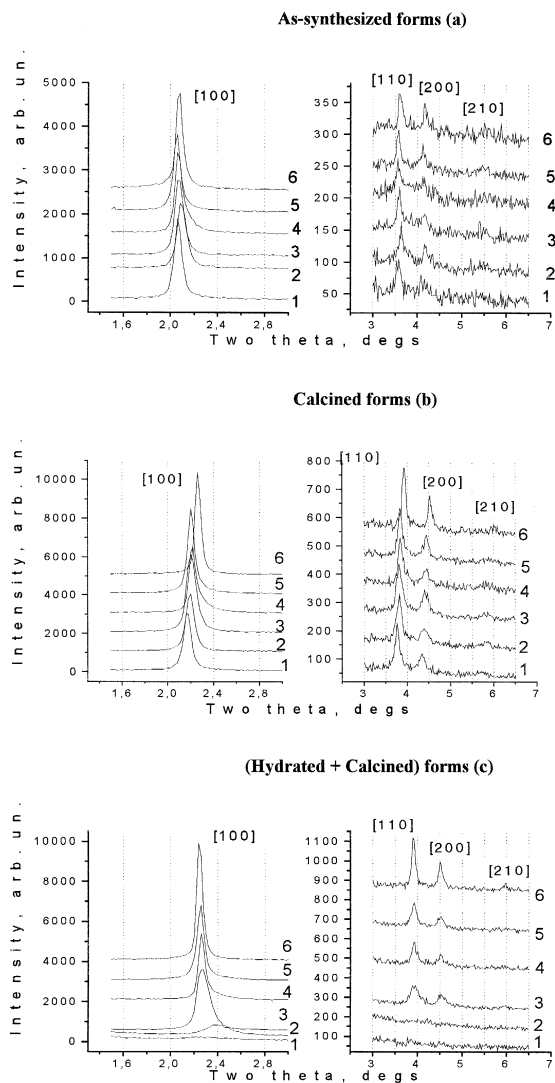


Fig. 1. The XRD patterns for as-synthesized (a), calcined (b) and (hydrated + calcined) forms (c) of the C16-(Si,Al)-MMM with the atomic portion of aluminium Al/(Si + Al) equals to: 0 (curves 1); 0.008 (curves 2); 0.02 (curves 3); 0.03 (curves 4); 0.04 (curves 5); 0.05 (curves 6).

terns allow us to describe the structure of all the samples in both as-synthesized and calcined forms as highly-ordered hexagonal arrangement of mesopores. Highly-ordered structure of the C16-(Si,Al)-MMM studied is indirectly supported also by a narrow interval of relative pressure $\Delta(P/P_0)$, within which the nitrogen capillary condensation occurs during low-tem-

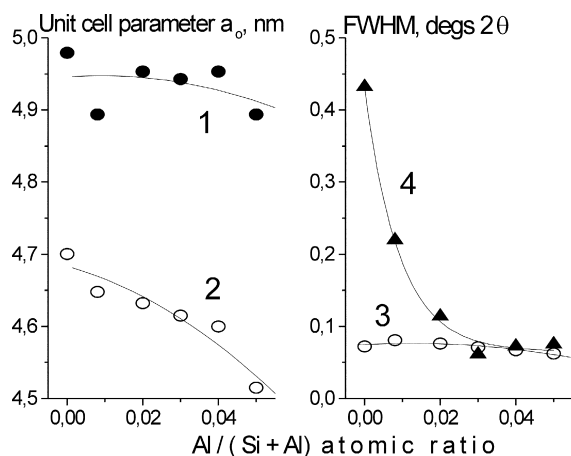


Fig. 2. Dependencies of the unit cell parameter and FWHM of the [100] reflection on the atomic portion of aluminium in the C16-(Si,Al)-MMM for as-synthesized (1), calcined (2,3) and (hydrated + calcined) forms (4).

perature adsorption, along with relatively small values of the external surface area (Table 1), calculated from the comparative graphs as described in Ref. [14].

All the above-mentioned observations permit us to consider unit cell parameters a_0 calculated from the XRD patterns as corresponding to exact values. As seen in Fig. 2, the a_0 value for as-synthesized forms is practically independent of the Al concentration (curve 1), whereas for calcined forms, this parameter decreases with increasing Al content, especially for the most concentrated samples (curve 2). Since it is known [14] that the lattice parameter for hexagonal arrangement can be expressed as a sum of

the mesopore diameter d_{Me} and the wall thickness h_w , a decrease of the a_0 value means a decrease in either the d_{Me} value, the h_w value, or both. Textural parameters of the samples from Table 1 help to clarify this problem. As seen from the Table, the h_w value remains almost unchanged (with a slight tendency to increase), while the d_{Me} value decreases noticeably with growing Al portion, especially for the samples with the highest Al concentration. This situation is schematically visualized in Fig. 3. It should be specially remembered that the structural changes described (Figs. 2 and 3) are observed under keeping constant both high intensity (Fig. 1) and very small FWHM value (Fig. 2, curve 3) of the [100] reflections.

Dramatic changes in the C16-(Si,Al)-MMM structure occur when calcined forms are hydrated with water vapour and then recalcined (Fig. 1c and Fig. 2, curve 4). As seen in the Figures, if the structure of low-concentrated samples collapses by degrees (the intensity of the [100] reflection decreases and its FWHM value increases) with decreasing Al concentration up to pure silica, while the structure of highly-concentrated samples remains practically unchanged. Indeed, as it was supposed earlier [15], the walls in pure siliceous C16-SiO₂-MMM consist of blocks, which are separated from each other with some gaps. At any rate, these blocks seem to be not fully bonded to each other even in the calcined material. As a result of such building-up of pure siliceous C16-SiO₂-

Table 1
Texture parameters of calcined forms of the C16-(Si,Al)-MMM samples

Al/(Si + Al) atomic ratio	$\Delta(P/P_0)^a$	Mesopore specific surface area (m ² /g)	External specific surface area (m ² /g)	Specific mesopore volume (cm ³ /g)	Mesopore diameter ^b (nm)	Wall thickness ^b (nm)
0	0.067	1065	44	0.930	4.05	0.66
0.008	0.076	1001	38	0.840	3.93	0.72
0.02	0.083	1016	53	0.875	3.95	0.69
0.03	0.077	1037	50	0.883	3.94	0.68
0.04	0.068	991	72	0.852	3.91	0.70
0.05	0.081	1013	76	0.831	3.81	0.70

^aRelative pressure range of nitrogen capillary condensation in mesopores during adsorption.

^bCalculated under assumption that $a_0 = d_{Me} + h_w$ as described in Ref. [14].

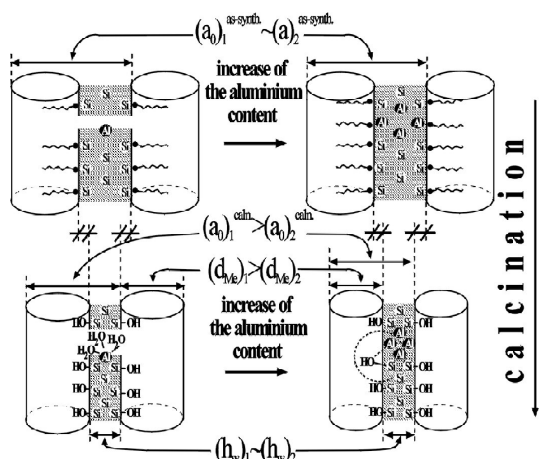


Fig. 3. Schematic representation of physico-chemical transformations during formation of mesoporosity in the C16-(Si,Al)-MMM.

MMM, its structure collapses almost completely when water, adsorbed on the preliminarily calcined form, is removed. This fact permits the supposition that aluminium atoms play a binding role ensuring a hydrostability of the C16-(Si,Al)-MMM.

In this connection it was important to elucidate coordination states of Al in the materials studied. As shown in Table 2, only tetrahedrally coordinated Al with practically constant NMR parameters is observed in as-synthesized forms. However, many changes in the ^{27}Al MAS NMR spectra were revealed for the samples after cal-

ination and full hydration. The appearance of the octahedral Al is the most important observation, increasing the total aluminium content, the smaller is the portion of this state. And terminal calcined sample contains no octahedral Al. Moreover, the integral NMR intensity decreases noticeably, and the width of the signal from octahedral Al increases strongly with growing aluminium concentration. Additional calcination (and following full hydration) of the samples does not result in any changes of the spectra parameters.

These facts mean that in samples of low concentration at least a part of Al atoms are localized so that aluminium is able to reach its coordination sphere up to octahedral, and, additionally, these atoms probably contain no Al atoms in their second coordination sphere since the corresponding NMR signal is very narrow (less than 100 Hz). If one admits that these isolated Al atoms are localized in the gaps of siliceous matrix (as it is shown in Fig. 3), then both a decrease of the integral NMR intensity and an increase of the width of the signal from octahedral Al (up to a complete disappearance of this signal) with growing total Al should be associated with filling up the above-mentioned gaps with aluminium–oxygen clusters.

Table 2

Main parameters of the ^{27}Al MAS NMR spectra for the C16-(Si,Al)-MMM samples

Al/(Si + Al) atomic ratio	As-synthesized forms				Calcined form				
	Al_T^a	I_{REL}^c (%)	Al_O^b	I_{REL}^c (%)	$I^{\text{CALN}}/I^{\text{AS-SYNTHC}}$ (%)	Al_T^a	I_{REL}^c (%)	Al_O^b	I_{REL}^c (%)
	$\Delta\nu^d$ (Hz)		$\Delta\nu^d$ (Hz)			$\Delta\nu^d$ (Hz)		$\Delta\nu^d$ (Hz)	
0.008	960	100	–	0	89	865	74	77	26
0.02	1010	100	–	0	82	894	77	183	23
0.03	1076	100	–	0	75	1068	80	212	20
0.04	1017	100	–	0	60	1033	84	250	16
0.05	1011	100	–	0	58	951	100	–	0

^aA signal with $\delta_T = 51.8\text{--}53.4$ ppm from aluminium in tetrahedral coordination.

^bA signal with $\delta_O = 0.8\text{--}0.9$ ppm from aluminium in octahedral coordination.

^cRelative ^{27}Al MAS NMR integral intensity observed as compared with that for the as-synthesized forms.

^dWidth of the NMR signal.

^eStandardized signal intensity.

Table 3

Catalytic properties^a of the calcined C16-(Si,Al)-MMM samples in benzene alkylation with iso-butene. BETA zeolite^b was studied for comparison

Al/(Si + Al) atomic ratio	Conversion (%)		Selectivity on benzene converted basis (mol%)		Selectivity on iso-butene converted basis (mol%)		
	Benzene	Iso-butene	<i>tert</i> -Butyl- benzene ^c	C ₁₁ ⁺ aromatics	<i>tert</i> -Butyl- benzene ^c	C ₁₁ ⁺ aromatics	C ₅ C ₁₂ olefins
<i>C16-(Si,Al)-MMM</i>							
0.008	0.5	32.4	80	20	12	4	84
0.02	1.2	37.9	74	26	21	10	69
0.03	1.2	39.3	74	26	21	14	65
0.04	1.3	42.2	70	30	25	13	61
0.05	1.4	43.3	66	34	21	17	62
<i>BETA zeolite^b</i>							
0.048	7.1	76.7	88	10	82	13	3

^a Experimental conditions: molar ratio of (benzene/iso-butene) = 10; WHSV = 1.1–1.3; $t = 150 \pm 3^\circ\text{C}$.

^b Zeolite-1 from Ref. [16] with concentration of strong protic centers ($\nu_{\text{OH}} = 3610 \text{ cm}^{-1}$) equals to 94 $\mu\text{mol/g}$.

^c Selectivity to iso-butylbenzene was negligible (much less than 1 mol%) for the C16-(Si,Al)-MMM samples and about 1 mol% for BETA zeolite.

The results of catalytic studies, which were obtained using (hydrated + calcined) forms of the C16-(Si,Al)-MMM having residual sodium contents not more than 0.005 wt.%, are summarized in Table 3. As seen, catalytic activity of the materials increases with growing Al concentration probably due to keeping the mesoporous structure unchanged and, consequently, to increasing accessibility of acid centers. But, at the same time, the activity of the C16-(Si,Al)-MMM in all the cases is about 5–6 times lower as compared with that for BETA zeolite, unlike the conclusion published recently [17]. If the above-made supposition on the aluminium–oxygen clusters formation with increasing Al content in the C16-(Si,Al)-MMM is valid, then the lowered activity of the materials should be associated with the lowered in them, either the concentration or the strength of protic acid centers.

4. Conclusion

If one adheres to a zeolite-like model of the formation of strong acid center as the “bridged” hydroxyl group, then it is necessary to stabilize

Al atoms in isolated state to realize high acid–base catalytic activity of the C16-(Si,Al)-MMM. Such a situation seems more likely to be achieved for relatively diluted systems. However, if Al concentration is relatively low, the C16-(Si,Al)-MMM exhibits significantly decreased hydrostability of its structure. This trouble may be easily overcome by increasing Al content. However, aluminium clusters formation (i.e. an appearance of Al atoms in its second coordination sphere) seems to accompany such increase. As a consequence, the acceptor ability of clustered aluminium toward oxygen atoms of the nearest silanol group will be decreased, and resulted concentration (or resulted strength) of the “bridged” hydroxyl groups will be noticeably lowered as compared with that for BETA zeolite of close chemical composition.

Acknowledgements

This investigation was supported by the Russian Foundation for Basic Research, Grant No. 98-03-32390, by the joint INTAS-RFBR Grant No IR-97-0676, and by the CNRS-RAS joint research program, Project No. 5015.

References

- [1] J.S. Beck, J.C. Vartuli, W.J. Roth, M.E. Leonowicz, C.T. Kresge, K.D. Schmitt, C.-T. Chu, D.H. Olson, E.W. Sheppard, S.B. McCullen, B. Higgins, J.L. Schlenker, *J. Am. Chem. Soc.* 114 (1992) 10834.
- [2] A. Corma, *Chem. Rev.* 97 (1997) 2373.
- [3] S. Biz, M.L. Occelli, *Catal. Rev.-Sci. Eng.* 40 (3) (1998) 329.
- [4] U. Ciesla, F. Schüth, *Microporous Mesoporous Mater.* 27 (1999) 131.
- [5] A. Corma, V. Fornes, M.T. Navarro, J. Perez-Pariente, *J. Catal.* 148 (1994) 569.
- [6] R. Schmidt, D. Akporiaye, M. Stöcker, O.H. Ellestad, *J. Chem. Soc., Chem. Commun.* (1994) 1493.
- [7] Z. Luan, C.-F. Cheng, W. Zhou, J. Klinowski, *J. Phys. Chem.* 99 (1995) 1018.
- [8] A. Tuel, S. Gontier, *Chem. Mater.* 8 (1996) 114.
- [9] R. Ryoo, C.H. Ko, R.F. Howe, *Chem. Mater.* 9 (1997) 1607.
- [10] J.-H. Kim, M. Tanabe, M. Niwa, *Microporous Mater.* 10 (1997) 85.
- [11] M. Chatterjee, T. Iwasaki, H. Hayashi, Y. Onodera, T. Ebina, T. Nagase, *Catal. Lett.* 52 (1998) 21.
- [12] D. Trong On, S.M.J. Zaidi, S. Kaliaguine, *Microporous Mesoporous Mater.* 22 (1998) 211.
- [13] M. Hunger, U. Schlenk, M. Breuninger, R. Gläser, J. Weitkamp, *Microporous Mesoporous Mater.* 27 (1999) 261.
- [14] V.B. Fenelonov, V.N. Romannikov, A.Yu. Derevyankin, *Microporous Mesoporous Mater.* 28 (1999) 57.
- [15] E.G. Kodenev, A.N. Shmakov, A.Yu. Derevyankin, V.N. Romannikov, *Russ. Chem. Bull.* (2000) in press.
- [16] V.N. Romannikov, K.G. Ione, *J. Catal.* 146 (1994) 211.
- [17] C. Perego, S. Amarilli, A. Carati, C. Flego, G. Pazzuconi, C. Rizzo, G. Bellussi, *Microporous Mesoporous Mater.* 27 (1999) 345.